Molecular Crystals and Liquid Crystals Science and Technology. Section A. Molecular Crystals and Liquid Crystals
Publication details, including instructions for authors and subscription information:
http://www.tandfonline.com/loi/gmcl19

A New Nonlinear Optical Method to Measure the Elastic Anisotropy of Liquid Crystals

E. Santamato [a] , E. Ciaramella [b] & M. Tamburrini [b]
[a] Dipartimento di Scienze Fisiche- Università di Napoli, Pad. 20, Mostra d;Oltremare, 80125, Napoli, Italy
[b] Fondazione Ugo Bordoni, via B. Castiglione 59, 00142, Roma, Italy
Version of record first published: 24 Sep 2006.

To cite this article: E. Santamato , E. Ciaramella & M. Tamburrini (1994): A New Nonlinear Optical Method to Measure the Elastic Anisotropy of Liquid Crystals, Molecular Crystals and Liquid Crystals Science and Technology. Section A. Molecular Crystals and Liquid Crystals, 241:1, 205-214

To link to this article: http://dx.doi.org/10.1080/10587259408029757

Mol. Cryst. Liq. Cryst., 1994, Vol. 241, pp. 205–214
Reprints available directly from the publisher
Photocopying permitted by license only

Printed in the United States of America

A New Nonlinear Optical Method to Measure the Elastic Anisotropy of Liquid Crystals

E. SANTAMATO

Dipartimento di Scienze Fisiche—Università di Napoli, Pad. 20, Mostra d'Oltremare, 80125 Napoli, Italy

and

E. CIARAMELLA and M. TAMBURRINI

Fondazione Ugo Bordoni, via B. Castiglione 59, 00142 Roma, Italy

(Received July 22, 1993; in final form July 28, 1993)

A new method to measure the elastic anisotropy of liquid crystals is presented. The method is based on the determination of the transverse spatial decay of the molecular director profile across the shadow region of a truncated laser beam intense enough to reorient the sample. The effective optical Kerr constant due to laser-induced reorientation is simultaneously obtained.

PACS numbers: 61.30.Gd, 42.65.-k, 64.70.Md

1. INTRODUCTION

It is well known that a continuous wave laser beam impinging on a Nematic Liquid Crystal (NLC) film can induce a change in the reorientation of the molecular director $\hat{\mathbf{n}}$.[1] In the case of homeotropic alignment and for normal incidence no reorientation can be induced until the laser beam intensity reaches a characteristic threshold value.[2,3] This phenomenon is known as the Optical Fréedericksz Transition (OFT). At oblique incidence, the reorientation process has no threshold and the sample exhibits a Giant Optical Nonlinearity (GON), due to the laser-induced change in the refractive index of the medium.[4,5] In the case of GON and for laser intensities not too high, the index change Δn seen by the laser beam is proportional to the light intensity I so that an effective optical Kerr constant n_2 can be defined according to the simple law

$$\Delta n = n_2 I. \tag{1}$$

The laser-induced optical reorientation is confined to a small region near the laser spot at the sample and decays outside. For this reason the reorientation process is strongly affected by the actual laser beam profile and, what is more important, all three elastic constants for splay, bend and twist of the material are simultaneously involved. This makes a crucial difference with respect to the reorientation of NLC produced with static electric or magnetic fields or with flow excitation. In the latter cases, in fact, the induced reorientation, being nonlocal, is almost uniform in space.

In this paper we show how to exploit the spatial decay of the molecular distortion induced locally by a focused laser beam to have direct information on the elastic constants of the material. Our results have been found in good agreement with the most recent measurements reported in the literature made with traditional electrooptical methods.[7]

2. THE EXPERIMENT

The experimental set-up is reported in Figure 1. In the experiment we used a thin film of $E7$, a NLC mixture from British Drug House at ambient temperature. The film thickness was determined to be 120 ± 5 μm by observing the sample from the side in a microscope and by measuring the distance between the internal edges of the containing glasses with a ruled eye-piece. The cover glasses have been coated with HTAB, a surfactant provided by BDH, for homeotropic alignment. The molecular reorientation was induced by a TM-polarized argon laser beam (λ = 515 nm) focused onto the sample at oblique incidence. The beam radius at $1/e^2$ intensity at the sample was measured to be 500 μm. The incidence plane was horizontal. In this way only the extraordinary wave was propagating in the film and GON could be observed. The sample was put in one arm of a Mach-Zehnder interferometer as shown in Figure 1. The two lenses L_1 and L_2 (f = 50 mm) are

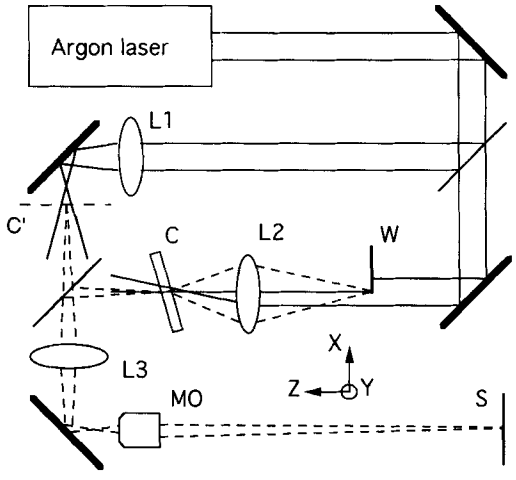

FIGURE 1 Experimental set-up. C, C' image planes conjugated to the screen S with respect to the microscope objective MO. At plane C is posed the nematic film of $E7$, 120 μm thick. L_1, L_2, L_3 lenses. W sharp edged blade.

at equal distance from the recombining beam-splitter, so that, in the absence of reorientation in the sample, two identical spherical wavefronts are superimposed at the exit of the interferometer. The imaging system is made by the lens L_3 (f = 50 mm) and by a 25X microscope objective MO and focuses on the screen S the interference pattern of the optical field distribution at planes C and C'.

With the laser at very low intensity and the sample present, the interferometer was slightly misaligned in order to obtain a pattern of equally spaced parallel fringes disposed horizontally or vertically on the screen (to measure the elastic constants in these two directions, respectively). Then a sharp edged blade was posed to intercept half of the laser beam in a plane behind the sample chosen so that the lens L_2 projected the blade image on the plane C. This could be easily checked, because when the blade is properly positioned its image is at focus on the screen S. Once the blade was positioned, the laser power was increased so that the resulting truncated Gaussian beam profile was intense enough to induce an appreciable molecular distortion in the liquid crystal. In about one minute the steady-state reorientation was achieved. At this point the blade was pulled off the beam and a photographic image of the inteference pattern on the screen was suddenly taken. A sample of such pictures is shown in Figure 2. The pictures were taken at laser power ranging from 300 to 350 mW and at different incidence angles. The two series correspond to the blade put along x and y, respectively. The difference in the spatial decay of the equal-intensity-lines in the two series can be seen by eye. It should be noted that the fringes in the region shadowed by the blade (on the right side of each picture in Figure 2) provide a useful reference frame of fringes. The distance of two consecutive fringes of this system corresponds to a difference of 2π in the optical phase and their position accounts only for the natural birefringence of the sample. The profile of the equal-intensity-lines yields therefore directly the value of the phase difference ψ due to the laser-induced index change as a function of the coordinate transverse to the beam and normal to the blade edge. The whole phase profile across the beam can thus be determined in absolute units. The effective optical Kerr constant n_2 of our sample was determined by measuring the laser-induced phase change in the absence of the blade and using the following definition relating the refractive index change to the phase change, viz.

$$\psi = \frac{2\pi L}{\lambda} \Delta n, \tag{2}$$

where L is the sample thickness and λ the laser wavelength in air.

3. DATA ANALYSIS

In order to obtain from the experimental data the elastic constants of the material we need a model for the laser-induced molecular reorientation. The laser intensity used in the experiment was low, so that the resulting molecular distortion in the

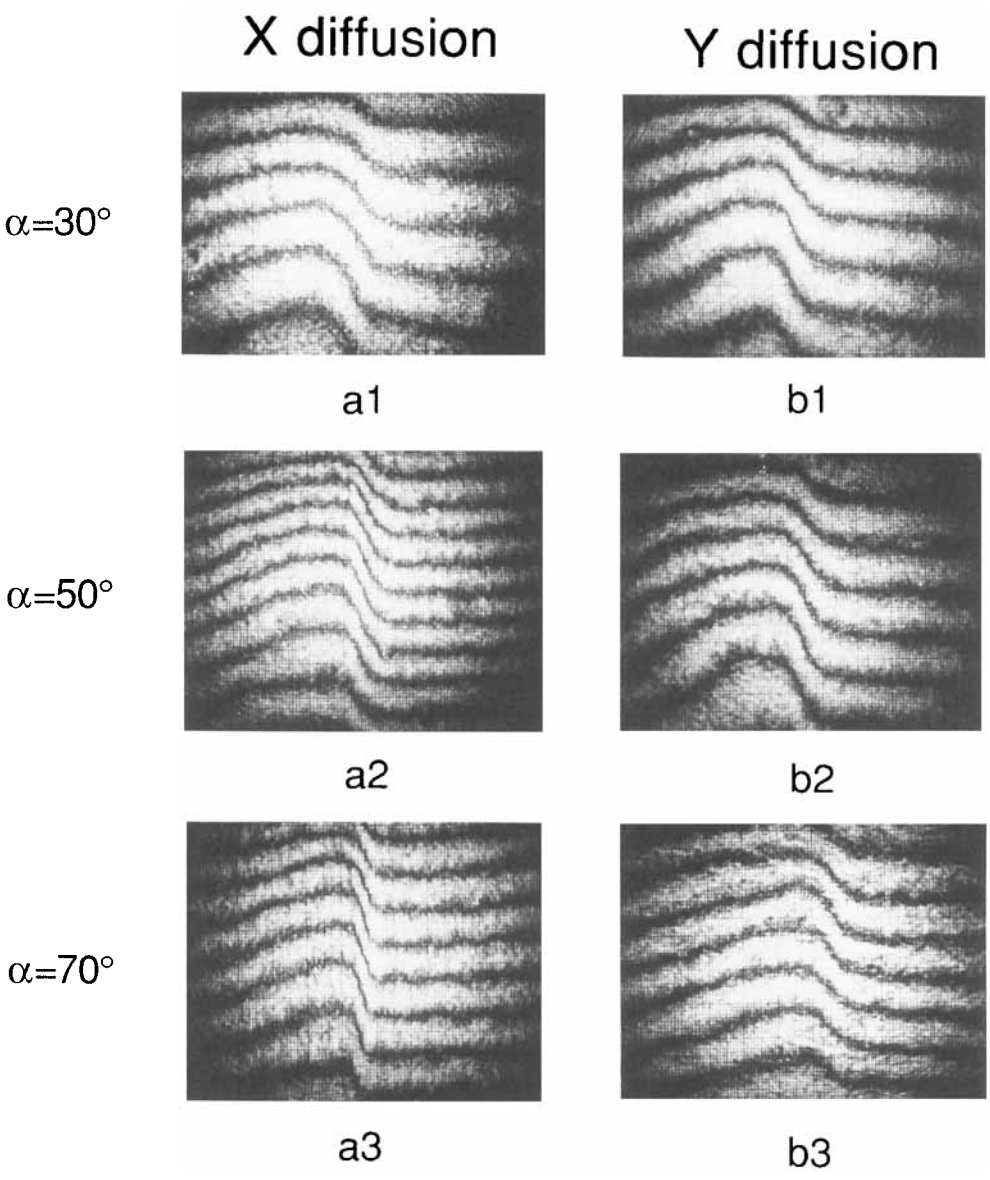

FIGURE 2 Fringe patterns on the screen. Figures a1, a2, a3 were obtained with the blade edge along the vertical y-axis at incidence angles of 30°, 50°, 70°, respectively. Figures b1, b2, b3 were taken at the same incidence angles, but with the blade along the horizontal x-axis.

sample was very small. For such small distortions the linearized laws governing the decrease of the director perturbation outside the light beam have been derived in Reference 5. In our geometry, where only the extraordinary wave is excited in the sample and the molecular director $\hat{\mathbf{n}} = (\sin\theta, 0, \cos\theta)$ lies in the incidence (x, z)-plane they read at steady-state

$$\left(\frac{k_{11}}{k_{33}}\right)\frac{\partial^2\theta}{\partial x^2} + \left(\frac{k_{22}}{k_{33}}\right)\frac{\partial^2\theta}{\partial y^2} + \frac{\partial^2\theta}{\partial z^2} + \left(\frac{\pi}{L}\right)^2\left(\frac{\sin\alpha}{\sqrt{\varepsilon_o}}\right)\left[\frac{I}{I_{Fr}}\right] = 0 \tag{3}$$

where

$$I_{Fr} = \frac{c\varepsilon_e k_{33}}{(\varepsilon_e - \varepsilon_o)\sqrt{\varepsilon_o}}\left(\frac{\pi}{L}\right)^2 \tag{4}$$

is the threshold intensity for the OFT at normal incidence (c is the light speed in vacuum and *cgs* units have been used). In Equations (3 and 4) $\varepsilon_e = n_e^2$ and $\varepsilon_o = n_o^2$, where n_e and n_o are the extraordinary and ordinary nematic refractive indices, k_{ii} ($i = 1, 2, 3$) denote the nematic elastic constants for splay, twist and bend, respectively, L is the sample thickness and α is the laser incidence angle in air. The intensity I appearing in Equation (3) is the projection of the incident intensity profile I_0 on the input face of the nematic film.

Observing that the phase change ψ due to the reorientation is given by

$$\begin{aligned} \psi &= \beta\langle\theta\rangle \\ \beta &= \left[\frac{2\pi(\varepsilon_e - \varepsilon_o)L}{\varepsilon_e\lambda}\right]\sin\alpha \end{aligned} \tag{5}$$

where $\langle\ \rangle = L^{-1}\int_0^L dz$ denotes the spatial average along the sample, we can convert Equation (3) into an equation for the phase change ψ, viz.

$$l_x^2\frac{\partial^2\psi}{\partial x^2} + l_y^2\frac{\partial^2\psi}{\partial y^2} - \psi + a\frac{I}{I_{Fr}} = 0 \tag{6}$$

where

$$\begin{aligned} l_x &= \frac{L}{\pi}\sqrt{\frac{k_{11}}{k_{33}}} \\ l_y &= \frac{L}{\pi}\sqrt{\frac{k_{22}}{k_{33}}} \\ a &= \frac{\sin\alpha}{\sqrt{\varepsilon_o}}\beta \end{aligned} \tag{7}$$

The numerical factors in the last equations arise from the z-dependence of the director polar angle θ across the film.[8] In our case the beam spot size at the sample was very large as compared to the film thickness, so that when the blade is absent, we may assimilate it to a plane wave. With the inserted blade edge along the

y-direction, say, we can approximate the intensity profile at the sample with the step function

$$I(x) = \begin{cases} I_0 \cos\alpha & x \leq 0 \\ 0 & x > 0 \end{cases} \tag{8}$$

Then Equation (6) can be easily solved yielding

$$\psi(x) = \begin{cases} \frac{1}{2}aI_0 \cos\alpha \left(2 - e^{-\frac{|x|}{l_x}}\right) & x \leq 0 \\ \frac{1}{2}aI_0 \cos\alpha e^{-\frac{|x|}{l_x}} & x > 0 \end{cases} \tag{9}$$

When the blade edge is along the x-direction, a similar equation holds, but with x replaced by y and l_x by l_y. The experimental data reported in Figure 3a have been therefore fitted with the formula

$$\psi(x) = C_1 \left[1 + \frac{(x - C_2)}{|x - C_2|}\left(e^{\frac{|x-C_2|}{C_3}} - 1\right)\right] \tag{10}$$

where C_1, C_2, C_3 are fitting parameters. A similar fit was made to the data in Figure 3b. The values of l_x^{meas} and l_y^{meas} as obtained from best fitting are reported in Figure 4 as functions of the laser incidence angle. Notice that the measured l_x^{meas} and l_y^{meas} are related to the quantities l_x and l_y in Equation (6) by the geometric factors $l_x^{\text{meas}} = l_x \cos\alpha$ and $l_y^{\text{meas}} = l_y$, due to the laser oblique incidence. The values of l_x and l_y have been therefore obtained by fitting l_x^{meas} and l_y^{meas} to $C \cos\alpha$, with C as fitting parameter, and to a constant, respectively. The best fit curves are dashed in Figure (4). The elastic constant ratios have been obtained by extrapolating l_x^{meas} to $\alpha = 0$. We found $l_x = 34$ μm and $l_y = 25$ μm, corresponding to the elastic constant ratios

$$\begin{aligned} \frac{k_{11}}{k_{22}} &= \left(\frac{l_x}{l_y}\right)^2 = 1.85 \\ \frac{k_{11}}{k_{33}} &= \pi^2 \left(\frac{l_x}{L}\right)^2 = 0.79 \end{aligned} \tag{11}$$

These ratios are in good agreement with the most recent determinations of the elastic constants of $E7$ as reported in Reference 7. In particular our ratio for k_{11}/k_{22} confirms very well the data reported in Reference 7, but it is in complete disagreement with earlier measurements,[9] which is essentially due to the large uncertainty of traditional techniques in measuring the twist constant k_{22}.

We measured also the ratio ψ/I_0 between the laser-induced phase change in the sample and the incident laser intensity. The effective optical Kerr constant n_2 was then obtained from Equations (1) and (2). The result is shown in Figure 5 for

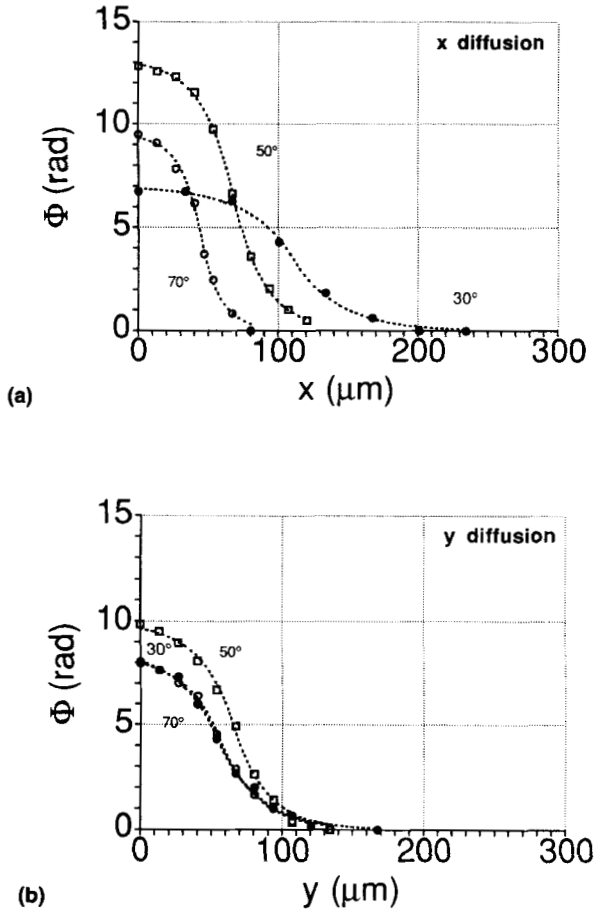

FIGURE 3 (a) Measured nonlinear optical phase change as a function of the x-coordinate across the beam at incidence angles of 30°, 50°, 70°. The blade edge was aligned along y. (b) Same as (a) but with the blade edge along x. Solid lines are the best fits with Equation (10).

different incidence angles. The data were taken without the blade and the phase change was measured at the center of the beam. For large beam, one can neglect the spatial second derivatives of ψ in Equation (6) and use the last of Equations (7) and (5) as well as Equation (4) to get n_2 as a function of the incidence angle α:

$$n_2 = \left(\frac{L^2}{\pi^2 c k_{33}}\right)\left(1 - \frac{n_o^2}{n_e^2}\right)^2 \sin^2 \alpha \cos \alpha \tag{12}$$

Using the optical index values $n_o = 1.524$ and $n_e = 1.732$ for $E7^{10}$ we can determine k_{33} by best fitting Equation (12) to the measured values of n_2. We found $k_{33} = 15.3\ 10^{-7}$ dyne, which is in very good agreement with the value of $k_{33} = 15.97\ 10^{-7}$ dyne as reported in Reference 7, especially if one takes into account that the present experiment was performed with no temperature control of the sample.

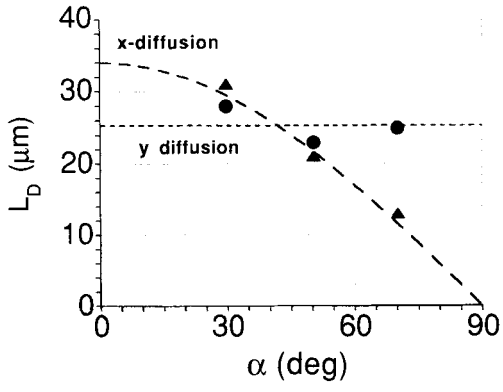

FIGURE 4 Values of l_x^{meas} and l_y^{meas} obtained from the best fit to the data reported in Figure 3 as functions of the incidence angle. The dashed curves are best fits to C cos α (C fitting parameter) for l_x^{meas} and to a constant for l_y^{meas}.

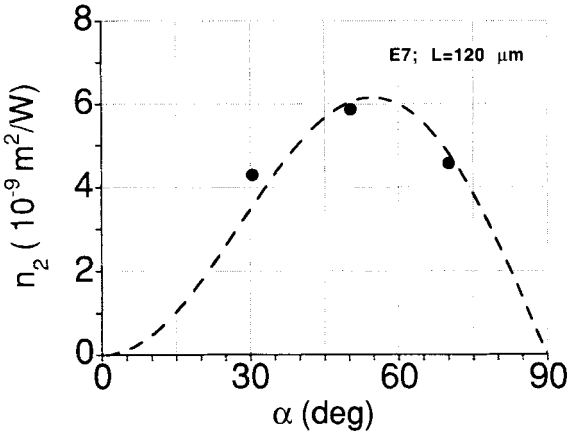

FIGURE 5 Measured effective nonlinear index n_2 of our sample as a function of the incidence angle α. The dashed curve is the best fit with Equation (12).

From the value of k_{33} and the measured elastic constant ratios [see Equations (11)] we get $k_{11} = 12.1\ 10^{-7}$ dyne, $k_{22} = 6.55\ 10^{-7}$ dyne, also in very good agreement with the values measured in Reference 7 with a completely different technique.

4. CONCLUSIONS

We presented a new nonlinear optical technique to measure the elastic constants of a nematic liquid crystal. The main advantage of this technique is that the three elastic constants are all measured at the same point in the sample and in the same environmental conditions. In this respect the present technique is similar to the well-known methods based on light scattering that also permit a simultaneous measurement of all elastic constants.[11] The light scattering techniques, however,

require sophisticated photon counting electronics and are affected by large errors due to the spurious contribution of the defects to the scattered light. This effect can be particularly strong in the low-frequency region of the noise spectrum, especially when one deals with thin samples (typically less than 50 μm). The technique used in this work is well suited for thin films, but, being nonlinear, requires a good stabilization of the laser source. Moreover, the nonlinear optical Kerr response of the medium can be obtained in the same experiment.

Several improvements of this technique can be envisaged. For example, one could measure the viscosity coefficients of the liquid crystal by measuring the decaying time of the fringe profile at laser turning off. Although the experiment was carried out at ambient temperature, nothing prevents that the sample could be placed into an oven to obtain data at various temperatures. Moreover, the fringe pattern on the screen could be recorded by a camcorder and sent directly to a computer for further elaboration. The simple model used here for data analysis can be also greatly improved by taking into account the exact profile of the truncated beam and the correct spatial distribution of the director $\hat{\mathbf{n}}$ across the sample. The whole problem is in fact linear, in the small distortion approximation, so that powerful numerical techniques as Fast-Fourier-Transform or hopscotch methods[12] could be used to integrate the relevant partial differential equations. Nevertheless, the very good agreement found in the present work with the elastic constant values reported in the most recent experiments confirms that the present technique is highly reliable despite the overall simplified assumptions made in the model. In particular, it seems that this method yields very accurate values of the twist constant k_{22}, which is usually very difficult to measure with other techniques.

Acknowledgment

This work was carried out in the framework of the agreement between the Fondazione Ugo Bordoni and the Istituto Superiore Poste e Telecomunicazioni with partial support by Consiglio Nazionale delle Ricerche. One of us (E.S.) acknowledges support from the special project MADOF by Consiglio Nazionale delle Ricerche and by Ministero della Ricerca Scientifica e Tecnologica.

References

1. For recent reviews on the laser-induced reorientation in liquid crystals see: N. V. Tabiryan, A. V. Sukhov and B. Zel'dovich, "The Orientational Optical Nonlinearity of Liquid Crystals," *Mol. Cryst. Liq. Cryst.*, **136**, 1–140 (1986); I. C. Khoo, "Nonlinear Optics of Liquid Crystals," *Progress in Optics*, XXVI, 107–161 (1988); F. Simoni, "Nonlinear Optical Phenomena in Nematics," in *Physics of Liquid Crystals*, Gordon & Breach, N.Y. 1989.
2. A. S. Zolot'ko, V. F. Kitaeva, N. Kroo, N. I. Sobolev and L. Csilag, *Pis'ma Zh. Exp. Teor. Fiz.*, **32**, 170 (1980) [*JETP Lett.*, **32**, 158 (1980)].
3. D. Durbin, S. M. Arakelian and Y. R. Shen, *Phys. Rev. Lett.*, **47**, 1411 (1981).
4. B. Ya. Zel'dovich, N. F. Pilipetskii, A. V. Sukhov and N. V. Tabirian, *Pis'ma Zh. Eksp. Teor. Fiz.*, **31**(5), 287 (1980) [*JEPT Lett.*, **31**, 263 (1980)].
5. B. Ya. Zel'dovich, N. V. Tabirian and Yu. S. Chilingarian, *Zh. Eksp. Teor. Fiz.*, **81**, 72 (1981) [*Sov. Phys. JEPT*, **54**(1), 32 (1980)].
6. B. Ya. Zel'dovich and N. V. Tabirian, *Zh. Eksp. Teor. Fiz.*, **82**, 1126 (1982) [*Sov. Phys. JEPT*, **55**(4), 656 (1982)].
7. H. L. Ong, M. Schadt and I. F. Chang, *Mol. Cryst. Liq. Cryst.*, **132**, 45 (1986).

8. We assumed a sinusoidal θ-profile along z and projected Equation (3) along the first spatial mode. This is a very usual approximation: see *e.g.* H. L. Ong, *Phys. Rev. A*, **28**, 2393 (1983).
9. M. Schadt and F. Müller, *IEEE Trans. Elec. Dev. ED*, **25**, 1125 (1978).
10. B. Bahadur, R. K. Sarna and V. G. Bhide, *Mol. Cryst. Liq. Cryst. Lett.*, **72**, 139 (1982).
11. See *e.g.* E. Miraldi, L. Trossi, P. T. Valabrega and C. Oldano, *Il Nuovo Cimento B*, **60**, 165 (1980) and references therein.
12. A. R. Gourlay, *J. Inst. Math. Appl.*, **7**, 216 (1971).